12-1-2011

Characterizing Performance of a PEM Fuel Cell for a CMET Balloon

Denise A. McKahn
Smith College, dmckahn@smith.edu

Whitney McMackin
Smith College

Proceedings of the ASME 2011 9th Fuel Cell Science, Engineering and Technology Conference
FuelCell2011
August 7-10, 2011, Washington, DC, USA

FuelCell2011-54532

CHARACTERIZING PERFORMANCE OF A PEM FUEL CELL FOR A CMET BALLOON

Denise A. McKahn and Whitney McMackin
Picker Engineering Program, Smith College, Northampton, MA, 01063
Contact e-mail: dmckahn@smith.edu

ABSTRACT

We present the design of a multi-cell, low temperature PEM fuel cell for controlled meteorological balloons. Critical system design parameters that distinguish this application are the lack of reactant humidification and cooling due to the low power production, high required power mass-density and relatively short flight durations. The cell is supplied with a pressure regulated and dead ended anode, and flow controlled cathode at variable air stoichiometry. The cell is not heated and allowed to operate with unregulated temperature. Our prototype cell was capable of achieving power densities of 43 mW/cm^2/cell or 5.4 mW/g. The cell polarization performance of large format PEM fuel cell stacks is an order of magnitude greater than for miniature PEM fuel cells. These performance discrepancies are a result of cell design, system architecture, and reactant and thermal management, indicating that there are significant gains to be made in these domains. We then present design modifications intended to enable the miniature PEM fuel cell to achieve power densities of 13 mW/g, indicating that additional performance gains must be made with improvements in operating conditions targeting achievable power densities of standard PEM fuel cells.

1 INTRODUCTION

There are two main categories of operating conditions for unmanned aerial vehicle (UAV) and unmanned aerial system (UAS) applications, those that require flight at either low (UASs) or high altitude (UAVs). Controlled meteorological (CMET) balloons are low altitude aerial systems used for the collection of weather data. The balloons require power for altitude control, sensors, data acquisition, data storage and communication [1]. In addition to altitude, flight time plays a critical role in power system design. A long endurance flight is widely regarded as having the capability of achieving continuous operation for up to 200 hrs, and typically occurs at high altitude [2]. Whereas low altitude flights, have mission lengths between 1-15 hours.

At both high and low altitude, several power system strategies have been employed, such as batteries [1], gas engines hybridized with batteries [3], photovoltaic panels hybridized with fuel cells [4], and even gas turbines hybridized with fuel cells [2]. For non-flight based applications, low temperature PEM stacks operating in the field have proven to provide reliable power for well over 3000 hours [5, 6]. This endurance, coupled with their electrical response time, and ability to startup at ambient, and even freezing [7] conditions, make PEM fuel cell power systems a suitable candidate for CMET balloons. The performance constraints of the fuel cell, however, vary considerable and will depend upon the operating conditions associated with oxygen partial pressure and temperature at flight altitude.

Miniature and micro fuel cells designed for low power output, ranging between 1-50 W, have been widely explored for portable electronics, where they are used as an alternative to battery technologies. The fuel cell active area approaches 8 cm^2 [8], with maximum power densities ranging from 20-190 mW/cm^2 [8]. This observed performance is an order of magnitude lower than that realized for fuel cells with active areas in the range of 100 cm^2 and larger. A range of limiting current densities, of 1.05-1.8 A/cm^2, was determined by [9] for a variety of PEM materials at standard operating conditions (60-80 ^{o}C, fully humidified flow through anode and cathode). In their work, this limitation was defined by induced cathode flooding (mass transport limitations)

and detected via neutron radiography.

What is not clear is whether the performance discrepancy between miniature and standard PEM fuel cells is a result of cell design or cell operating conditions (system architecture). This work presents an evaluation of miniature PEM fuel cell system architectures that specify cell operating conditions. This discussion is followed by the presentation of a detailed miniature fuel cell design, testing and performance evaluation. Specifically, we distinguish the gains in polarization performance that can be made due to cell design from those associated with operating performance. Here, we focus on low altitude and ultra-lightweight CMETs (UASs), with high energy density, low total power production, and few volumetric constraints as an alternative to batteries.

2 SYSTEM ARCHITECTURE

The power demands of lightweight aerial systems are driven by on-board instrumentation and navigation requirements. A significant constraint relates to the total system mass, imposing high energy mass-density constraints on the power and fuel storage and delivery systems. Thus, a high net system electrical efficiency is needed to reduce the mass of fuel required on board. With respect to operating conditions, the fuel cell stack must be able to startup at ambient temperature and pressure conditions at the altitude at which power is demanded.

The configuration of the anode has a significant influence on cell water management. When supplying reactants to the anode in excess of the reaction rate, referred to as flow through operation, the supply gasses must be humidified and well regulated with appropriate feedback control. An example of typical hardware deployed for a flow through anode is shown in Figure 1. An undesirable consequence of flow through operation is that excess reactants are lost unless additional equipment is used to recirculate the anode exhaust gases back to the inlet. A flow through configuration is common for laboratory testing where precise control of the anode operating conditions is desired, or during operation with a reformate fuel mixture that contains some fraction of impurities, such as methane or carbon dioxide. With flow through operation, water is not likely to accumulate on the anode and can be regulated through stoichiometric control at the anode inlet.

Dead ended anode operation has proven to be an effective and simple anode configuration when supplying pure hydrogen [5, 6, 10], where anode reactants are supplied at the reaction rate through pressure regulation rather than flow control, as shown in Figure 1. With a dead-ended anode, a purge solenoid is located downstream of the anode and periodically opened to remove any water or impurities that have accumulated on the anode. Purging periodicity can be a function of the cell current density, temperature, cathode air stoichiometry, or simply operating time. Water flooding will dominate on the anode at low current densities (¡100mA/cm^2), and at the cathode at high current densities [11]. Specifically, flooding occurs when back diffusion dominates electroosmotic drag [12]. While dead ended operation eliminates the need for humidifying the hydrogen gas supplied to the anode (significantly reducing system weight), as well as the need for a flow controller, the occurrence of anode flooding requires appropriate control strategies to remove liquid water. A common and simple strategy involves purge scheduling, however, more sophisticated strategies, such as exhaust gas recirculation with a condenser [13], have been considered.

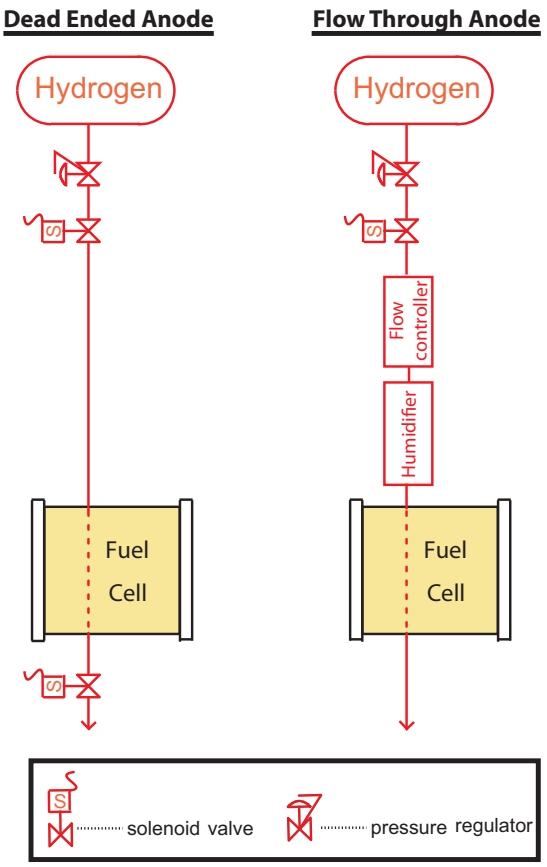

Figure 1. Standard hardware for dead ended (pressure controlled) vs flow through (flow controlled) anode reactant delivery.

With respect to onboard fuel, significant investment in hydrogen storage has focused on weight constraints, with recent advances in carbon fiber composition and structure, as well as lightweight metal hydrides. Unfortunately, due to the low fuel cell operating power, fuel cell waste heat cannot be used to release hydrogen gas from hydride storage vessels, making metal hydrides an impractical storage option for small low altitude aerial systems. However, unlike portable electronics, the volume of the hydrogen storage containment system is not critical for UASs. Rather, weight poses the limiting constraint. Consid-

ering that hydrogen can be stored at low pressure (supplying gas to the anode at slightly above atmospheric and greater than the total pressure observed at the cathode), the containment vessel does not need to tolerate high pressure nor leverage porous hydride structures for hydrogen sorption. Therefore, in this specific application, there is a potential for significant weight reductions to the hydrogen storage system that have not yet been fully evaluated.

To reduce or omit the electrical losses in supplying forced air to the cathode, several researchers have considered air breathing fuel cells, at the expense of water removal. To examine these tradeoffs, [14] experimentally manipulated heat and mass transfer material properties to characterize the ratio of heat and thermal resistances for which dehydration or flooding occur in air breathing cells. In achieving high limiting current densities, they recommend reducing thermal resistances and increasing mass transport resistances to increase the current density at which the cell transitions from flooding to dehydration. This recommendation, however, results in a greater need for water management with increased cathode water production rates at these higher current densities. [15] proposed a cover with a variable opening area to dynamically change the fraction of exposed cathode surface area, resulting in a means of regulating oxygen partial pressure, membrane water content, and the boundary of flooding and dehydration as cell temperature fluctuates. While this was achieved with scotch tape, their work merits a more detailed analysis, as shown with sliding plates as a means for active humidification in larger PEMFC stacks [16].

Several strategies have been employed to humidify PEM fuel cell reactants, in an attempt to maintain the desired membrane hydration state. Membrane-type humidifiers [17] are either internal [18–20] or external [21] to the PEM fuel cell stack. These membrane humidifiers, however, utilize hot coolant as the water source, an option not available for low power CMET applications. Humidified reactant exhaust streams can instead be used to heat and humidify the incoming reactants [22]; however, the ability to achieve desirable relative humidities at the reactant inlets will be constrained by the cell operating temperature and thermal gradients between the power and humidification portions of the stack. This humidification strategy, also referred to as air-to-air humidification, while considered extensively for high power applications, has not yet been rigorously evaluated for miniature fuel cells.

The simplest operational strategy was chosen for the CMET prototype system. The fuel cell operates with no reactant pretreatment (humidification), a dead ended and pressure controlled anode, and a flow controlled cathode. A schematic of the major system components is depicted in Figure 2, specifically targeting experimentation. When the fuel cell is deployed on the balloon, the air compressor would be replaced with a miniature air pump. Dry pure hydrogen is pressure regulated at the anode inlet to 3 psig (1.2 bar). This pressure regulation system replenishes the hydrogen consumed in the chemical reaction. For the majority of the operational time, the hydrogen stream is dead-ended with no flow external to the anode. Using a purge valve located downstream of the anode, hydrogen can be momentarily purged through the anode to remove water and gases. The mass flow rate of dry air is provided to the cathode at a desired stoichiometric ratio.

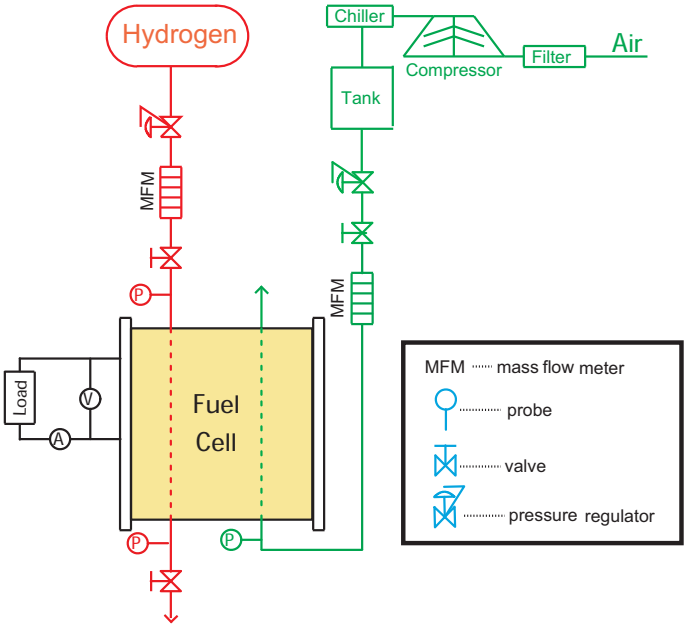

Figure 2. Fuel cell experimental hardware.

3 CELL DESIGN

Each cell was comprised of a conductive and relatively impervious flow field separator plate, Buna-N gaskets, gas diffusion layers (GDL), and a membrane electrode assembly (MEA). Endplates were used to apply a compressive force to the cells using tie-rods. This section describes the choices made in material selection and design. Due to the large number of CMET balloons that could be launched in a single campaign, standard off the shelf components were deemed to be more desirable than custom fabricated components if these standard components proved to have relatively similar performance. A summary table of the component masses is provided in Table 1.

3.1 MEA and GDL

The fuel cell utilizes standard commercially available MEAs purchased from Ion Power. These MEAs consist of a Nafion 111 membrane electrode assembly, an active area of 5.5 cm^2, a catalyst layer of 0.3 mg/cm^2 Pt/C on the anode and cathode with integrated Kapton gaskets.

The selection of the gas diffusion layers (GDL) employed in the cell can have a considerable consequence for cells that oper-

Table 1. Cell component masses.

Part	**Mass**(g)
Cathode Flow Field	36.16
Anode Flow Field	37.53
Endplate Gasket	2.12
GDL Gasket	0.68
Anode Endplate w/fittings	14.02
Cathode Endplate w/fitting	13.5
Tie-rods and nuts	1.69
GDLs	0.26

ate at high current density. In comparing the use of microporous layers (MPLs) with carbon cloth based GDLs, [23] found that there is better voltage performance and lower membrane resistance (related to increased hydration) when the MPL is omitted if the cell is operated under dry conditions (as is the case for our UAS application), irrespective of current density. With non-woven GDLs operated under dry conditions, there is no significant difference in performance related to the use of MPLs at current densities less than 200 mA/cm^2 [23]. Additionally, under dry conditions, the performance of the carbon cloth versus the non-woven GDL were comparable at low current density [23]. Because non-woven carbon papers are easier to physically assemble into fuel cells as a result of their rigidity, and because the cell current density for our UAS is less than 200 mA/cm^2, a non-woven SGL Sigracet 10BB GDL was chosen with an uncompressed thickness of 0.38mm. Should higher current density operation be realizable under dry conditions, a non-woven carbon paper was recommended for UASs with a PTFE coating [23].

3.2 Separator Plates

Although aluminum is attractive due to its low mass, without a corrosive resistant coating, aluminum and its alloys have been observed to leach ions in an acidic environment, negatively affecting the output of the cell [24]. Various stainless steel alloys including 316 stainless steel have been found unsuitable for separator plate use due to the lack of corrosion resistance as well as the contact resistance being too high for acceptable performance for longterm operation [25]. Many multi-cell PEM fuel cell designs leverage graphite that is pyrolytically coated, resin-impregnated, or comprised of a composite which renders the plate impervious to gas flow through the pore structure. This graphite material choice is made due to the corrosion resistance required for relatively long (>4000 hours) stack life times as well as the low mass densities achieved at the expense of reduced strength and added manufacturing complexity. We elected to use flow field separator plates made of 316 stainless steel, due to their ability to be easily procured and machined with relatively quick lead times. Coating these stainless steel plates was unnecessary due to the low risk of corrosion during the short lifetimes expected of UASs, as well as the reduced cost and lead times. Mass comparisons between the use of stainless steel and graphite will be discussed in Section 4.

3.3 Gas Flow Channels

When considering the design of the gas distribution channels machined into the separator plates, there are two particular design choices to be resolved, channel orientation and channel dimensions. With respect to reactant distribution, miniature fuel cells have relatively narrow and shallow channels and thin plates due to space and/or weight constraints. With miniature fuel cells there is greater flexibility in channel orientation because uniform flow distribution can be easily achieved due to their small active area.

Interdigitated, serpentine, parallel and mesh channel designs with channel widths of 300um (0.012") and channel depths of 200 um (0.007"), were compared by [26] at ambient temperature. They found little difference in water accumulation between these flow patterns, with each approaching a channel blockage of between 40-50% and with all four exhibiting the same dynamic response (first order). Their work suggests that there is little benefit with respect to water management in selecting a particular channel design. Therefore, straight parallel channels were employed on the cathode and anode for simplicity.

Channels depths for miniature fuel cells were found to be between 100-400μm [8], as opposed to an order of 1000μm seen with standard PEMFCs. Smaller channels cause accumulated liquid water to more readily occlude channels. The occurrence of cathode flooding typically not observed until higher current density operation will, therefore, be more pronounced in miniature fuel cells, setting a lower constraint on the range of operable current densities [9] as well as a tradeoff between space constraints and water management [27]. Moreover, the Peclet numbers are not sufficient for liquid water detachment through convection [28], a serious limitation for air breathing fuel cells [9]. As a result, channel depths common for standard PEMFCs were employed in this work.

Figure 3 displays the flow patterns used for both the anode and cathode separator plates. Each channel was machined to a depth of 1.02mm and a width of 1.52mm with the channel lands and grooves evenly spaced and parallel. The internal manifolds used to distribute gas between cells are shown at the entrance and exit of each of the channels. The small holes located at the corners of the plates are used to pass tie-rods through each cell.

3.4 Endplates and Compression

Four tie-rods were used to hold the cell materials together and applied a clamping pressure of approximately 85 psi at the

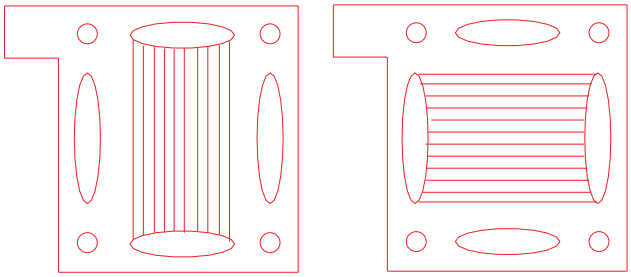

Figure 3. Separator plate design indicating the flow patterns for both the anode and cathode.

corners of the stack. This clamping pressure was measured using Ultra Low Fujifilm Prescale pressure sensitive paper and indicated uniform compression across the active area. To reduce weight, acrylic endplates were selected along with PTFE tierods and bolts. Initially, acrylic sheets with a thickness of 3.2mm (1/8") were selected, however these sheets warped (became concave) upon assembly. As a result, 6.4mm acrylic was used in the final design. It is important to note, the mass of the endplates is relatively insignificant (4%) when considering the total stack mass for a multi-cell stack. Thus, cell compression is of utmost importance in selecting materials and clamping mechanisms.

4 CELL PERFORMANCE

The CMET PEM fuel cell described in Section 3 was tested on an experimental test bench with the hardware configuration presented in Figure 2. Here we present the fuel cell performance data along with a modeling analysis of the influence of operating conditions on cell performance.

4.1 Membrane Water Content

For the application of CMET balloons, due to the aforementioned system weight constraints, characterizing cell performance under low membrane hydration conditions is critical to evaluating the tradeoffs associated with system weight and performance. Here we compare two voltage models and evaluate their ability to capture the influence of low membrane water content on cell voltage performance. First, to compare the ability of these two voltage models to capture the cell polarization of the CMET fuel cell, the membrane relative humidity must be known. While both the anode and cathode reactant supplies are dry, the production of water at the cathode requires a detailed numerical model to predict the transport of water within the cell structure.

The numerical model employed was developed and experimentally validated to characterize the performance of a 300cm^2 24 cell PEM fuel cell stack under anode flooding conditions when operated with a dead ended anode [10]. This model assumes the cell operates under isothermal conditions, an assumption that while limited for large stacks operating at high current density, is an adequate assumption for the CMET fuel cell which operates near ambient temperature and has a relatively small active area. The model characterizes two phase flow through a spatially distributed gas diffusion layer with a single volume membrane and catalyst layer.

As described in Section 2, the cell is operated with a dry supply of air and hydrogen ($\phi_{ca,in} = \phi_{an,in} = 0$), ambient temperature ($T_{cell}$=20^{o}C) due to low current density operation, and 300% air stoichiometry. The model described in [10] was adjusted to predict cell performance for a 5.6 cm^2 single cell under the experimental test conditions described here. Under these conditions, the cell was predicted to have membrane water contents as low as λ=3 H_2O/SO_3^-, with little sensitivity to cell operating temperature. Of critical influence, as expected, is the cathode inlet humidity, air stoichiometry, electrode volumes and purging schedules.

4.2 Cell Polarization

While steady-state polarization measurements do not offer a conclusive data set for predicting transient phenomena such as electrode flooding [10, 29] or hysteresis, they provide a useful characterization when predicting the steady influence of cell operating conditions such as temperature, pressure and humidity. The cell voltage, v, is equal to the theoretical open circuit voltage, E, minus the activation, v_{act}, and ohmic, v_{ohmic}, losses such that

$$v = E - v_{act} - v_{ohmic} \, . \tag{1}$$

Here we neglect to model the concentration overvoltage associated with a mass transport limitation at high current density due to our operation at relatively low current densities ($i < 0.4$ A/cm^2).

When chemical potential is related to concentration through activity in a nonreversible system, the theoretical open circuit voltage varies with respect to reactant partial pressures and temperature. This variation is expressed through the change in Gibbs free energy and the Nernst Equation [30]. The activation overvoltage accounts for both the forward and reverse activation barriers through the Butler-Volmer Equation to reflect the concentration dependence of the exchange current density [30]. Modifying the Butler-Volmer equation to also account for the the loss current density resulting from the transport of molecular hydrogen from the anode to the cathode through the membrane [31], the total activation voltage loss can be described. There is little dispute over these mathematical models, described by

$$E = -\left(\frac{\Delta H}{2F} - \frac{T_{cell}\Delta S}{2F}\right) + \frac{RT_{cell}}{2F} \ln\left(\frac{p_{H_2,an}\sqrt{p_{O_2,ca}}}{(p_o)^{1.5}}\right), \tag{2}$$

$$v_{act} = K_1 \frac{RT_{cell}}{2F} \ln\left(\frac{i+i_{loss}}{i_o}\right), \quad (3)$$

$$i_0 = K_2 \left(\frac{p_{O_2,ca}}{p_o}\right)^{K_3} \exp\left[-\frac{E_c}{RT_{cell}}\left(1-\frac{T_{cell}}{T_o}\right)\right], \quad (4)$$

where ΔS and ΔH are the differences in entropy and enthalpy from standard state conditions, p_o is the standard pressure, the oxygen and hydrogen partial pressures, $p_{O_2,ca}$ and $p_{H_2,an}$, are located either at the GDL surface in contact with the catalyst layer, or within the catalyst layer, T_{cell} is the cell operating temperature, F is Faraday's constant, R is the universal ideal gas constant, K_1-K_3 are tunable parameters (K_1 is the reciprocal of the charge transfer coefficient), i_{loss} is the loss current density due to hydrogen crossover, i is the current density, i_o is the exchange current density [31],E_c is the activation energy for oxygen reduction on Pt, and T_o is the reference temperature.

Of greatest importance to our task of characterizing cell voltage performance under low humidity conditions is consideration of the ohmic voltage loss. Charge transport is dominated by membrane ionic conductivity, as well as contact and bulk electrical resistance of the electrically conductive materials [30]. The cells considered in this work do not operate at significant pressure gradients, thus convective transport is neglected. Generally, the ohmic voltage loss is expressed as a linear function of this charge transport resistance with a variety of functional relationships having been posed depending upon the cell operating conditions.

A widely used model for capturing the influence of membrane water content and temperature on membrane conductivity was originally presented in [32] where the ionic conductivity is a linear function of membrane water content at 30^{o}C, with the following functional form,

$$v_{ohmic} = K_4 \left[\frac{t_{mb}}{(b_{11}\lambda_{mb} - b_{12})} e^{-1268\left(\frac{1}{303}-\frac{1}{T_{cell}}\right)}\right] i, \quad (5)$$

where K_4 is a tunable parameter, t_{mb} is the membrane thickness, b_{11} and b_{12} are experimentally identified parameters from [32], and λ_{mb} is the membrane water content. Here, the ionic resistance is assumed to dominate the electrical resistance, thus electrical resistance has been neglected.

Neglecting the influence of temperature in air breathing PEM fuel cells, [14] posed a different ohmic voltage loss,

$$v_{ohmic} = \left(AR_{electric} + \frac{t_{mb}}{\sigma_{RH}}\right) i, \quad (6)$$

where σ_{RH} is the membrane conductivity as is described by a polynomial function of membrane relative humidity ($\sigma_{RH} = 7.46\phi_{mb}^3 - 7.45\phi_{mb}^2 + 3.13\phi_{mb} - 0.378$), $R_{electric}$ is the cell electrical resistance, and A is the membrane active area. This particular model could be best suited for low temperature CMET applications. Unfortunately, this relationship for membrane conductivity has a root at ϕ_{mb}=0.19, indicating that the ohmic overpotential would be a gain rather than a loss at low humidity. Thus, this model is not appropriate for low membrane humidities (water contents). The main distinction between these two models is in the mathematical order of the relationship between membrane conductivity and membrane water content (humidity) and the inclusion of temperature effects.

4.3 Testing Results

Upon assembly the fuel cell membrane was pre-soaked with de-ionized water. The cell was then placed on the test bench with a sequence of polarization data taken over a period of one hour, operating at a constant resistance of 5 Ω between each polarization sweep. Because the fuel cell will be operating under low humidity conditions with a relatively short lifetime, the membranes were not pre-conditioned.

Figure 4 displays the modeled influence of membrane water content on cell polarization, using the ohmic voltage loss presented in Equation 5, alongside the experimental data. To compare these two models, the voltage parameters were identified, as shown in Table 2, using linear least squares to minimize the difference between the measured and modeled cell voltage if the membrane water content were λ=4 H_2O/SO_3^-.

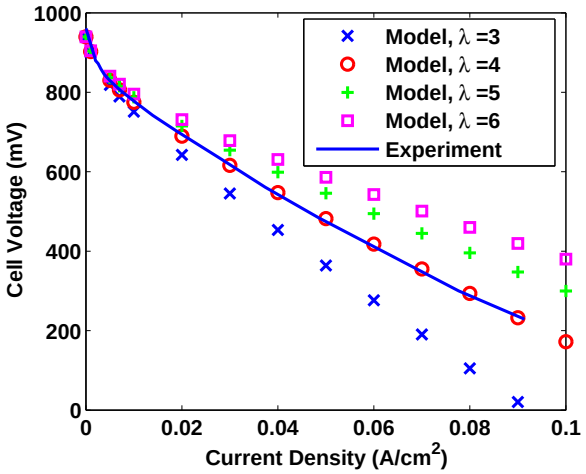

Figure 4. The influence of membrane water content, λ in H_2O/SO_3^-, on modeled cell polarization along with the experimental data.

When operating at the maximum power point, this cell is capable of producing 43 mW/cm^2 and 5.4 mW/g, within the range expected for miniature PEM fuel cells. As expected, similar cell

Table 2. Voltage Model Parameters.

Parameter	Value	Units
ΔH	-241980	J/mol
ΔS	-44.43	J/mol K
T_o	298.15	K
p_o	101325	Pa
E_c	$66x10^3$	J/mol
i_{loss}	0.001	A/cm^2
b_2	1268	
b_{11}	0.005139	
b_{12}	0.00326	
t_{mb}	0.00381	cm
K_1	1.8	
K_2	-21.5	
K_3	2.05	
K_4	22	

performances were observed for a variety of flow channel designs including serpentine flow. Cell channels of less depth, decreased from 1mm down to 0.25mm, showed little influence on cell polarization. Channel distribution differences were also explored, using perforated metal and screen mesh, also with little observable difference in cell performance.

To investigate the influence of dead-ended anode operation, the cell was run for 5 minutes at different loading levels starting at 13 mA/cm^2 and ending at 44 mA/cm^2 for a total of 20 minutes of operation. The load level was changed every 5 minutes and the cell was purged before each change in load. Following the anode purge, cell voltage had no response, indicating both a lack of water or nitrogen accumulation at the anode. As a result, dead-ended anode operation is deemed suitable for this UAS application.

Given the cell polarization performance shown in Figure 4, the performance data can be scaled to size a fuel cell stack comparable to the Lithium Ion batteries currently used for the CMET balloons in [1]. The target stack voltage is 3.7 VDC (V_{cell}=0.465 VDC), resulting in 8 cells/stack operating at 500mA (92 mA/cm^2). The total stack mass would be 380g, with a power density of 43 mW/cm^2/cell or 5.4mW/g. If graphite were used, rather than stainless steel, for the bipolar separator plates (flow fields), the power density could be further increased to 13 mW/g (a stack mass reduction to 140 g). While this material choice is clearly significant, the target power density still falls well below that of the Lithium Ion batteries (66 mW/g). Given cell performance, the stack mass would need to be reduced to 28 g, in order to compete with batteries.

A typical, 50 cm^2 low temperature PEM fuel cell operating with a dead-ended dry anode, the same MEA, GDL, channel depths, channel widths and channel layout, along with graphite separator plates, a fully humidified cathode operating at 60^{o}C experimentally exhibits a conservative cell performance of 250 mW/cm^2/cell (0.5 VDC at 500 mA/cm^2). This improved performance suggests the significant gains that can be made with high temperature and humidity conditions. With this performance (under humidified conditions), and the mass expected for the miniature fuel cell stack (140 g), power mass-densities exceeding that of batteries (70 mW/g) could be achieved. Thus, a thorough investigation into the tradeoffs associated with improving the operating conditions is warranted along with consideration of membranes that can tolerate low humidity conditions.

5 CONCLUSIONS

A prototype PEM fuel cell, designed and constructed for CMET applications, was capable of maintaining 43 mW/cm^2/cell or 5.4 mW/g. Choosing graphite bipolar separator plates, as opposed to stainless steel plates, could further improve this performance to 13 mW/g. However, the stack masses needed to compete against Lithium Ion batteries, suggest that significant improvements must be made in the cell operating conditions. To improve ohmic losses, cell temperature and membrane water content must be increased without sacrificing weight.

REFERENCES

[1] Riddle, E., Voss, P., Stohl, A., Holcomb, D., Maczka, D., Washburn, K., and Talbot, R., 2006. "Trajectory model validation using newly developed altiture-controlled balloons during the international consortium for atmospheric research on transport and transformations 2004 campaign". *Journal of Geophysical Research,* **111**.

[2] Aguiar, P., Brett, D., and Brandon, N., 2008. "Solid oxide fuel cell/gas turbine hybrid system analysis for high-altitude long-endurance unmanned aerial vehicles". *International Journal of Hydrogen Energy,* **33**.

[3] Harmon, F., Frank, A., and Joshi, S., 2005. "The control of a parallel hybrid-electric propulsion system for a small unmanned aerial vehicle using a cmac neural network". *Neural Networks,* **18**.

[4] Cestino, E., 2006. "Design of solar high altitude long endurance aircraft for multi payload and operations". *Aerospace Science and Technology,* **10**.

[5] Chamberlin, C., Lehman, P., Zoellick, J., Engel, R., and Rommel, D., 2002. "Fuel cell/photovoltaic integrated

power system for a remote telecommunications station". In Proceedings of the 2002 Fuel Cell Seminar.

[6] Lehman, P., Chamberlin, C., Chapman, G., Coleman, N., Engel, R., McKay, D., Marshall, M., Reis, A., and Zoellick, J., 2002. "Field testing of a pem fuel cell in an integrated power system". In Proceedings of the 2002 Fuel Cell Seminar.

[7] Pesaran, A., Kim, G.-H., and Gonder, J. "Pem fuel cell freeze and rapid startup investigation". In *Milestone Report NREL/MP-540-38760*.

[8] Kundu, A., Jang, J., Gil, J., Jung, C., Lee, H., Kim, S.-H., Ku, B., and Oh, Y., 2007. "Micro-fuel cells - current development and applications". *Journal of Power Sources,* **170**.

[9] Seyfang, B., Boillat, P., Simmen, F., Hartmann, S., Frei, G., Lippert, T., Scherer, G., and Wokaun, A., 2010. "Identification of liquid water constraints in micro polymer electrolyte fuel cells without gas diffusion layers". *Electrochimica Acta,* **55**.

[10] McKay, D., Siegel, J., Ott, W., and Stefanopoulou, A., 2008. "Parameterization and prediction of temporal fuel cell voltage behavior during flooding and drying conditions". *Journal of Power Sources,* **178**.

[11] Karnik, A., Stefanopoulou, A., and Sun, J., 2007. "Water equilibria and management using a two-volume model of a polymer electrolyte fuel cell". *Journal of Power Sources,* **164**.

[12] McKay, D., and Stefanopoulou, A., 2004. "Parameterization and validation of a lumped parameter diffusion model for fuel cell stack membrane humidity estimation". In IEEE Proceedings of 2004 American Control Conference.

[13] Karnik, A., Sun, J., and Buckland, J., 2006. "Control analysis of ejector based fuel cell anode recirculation system". In Proceedings of the 2006 American Control Conference, Vol. 164.

[14] Paquin, M., and Frechette, L. G., 2008. "Understanding cathode flooding and dry-out for water management in air breathing pem fuel cells". *Journal of Power Sources,* **180**.

[15] Karst, N., Faucheux, V., Martinent, A., Bouillon, P., Laurent, J.-Y., Druart, F., and Simonato, J.-P., 2010. "Innovative water management in micro air-breathing polymer electrolyte membrane fuel cells". *Journal of Power Sources,* **195**.

[16] Chen, D., and Peng, H., 2005. "A thermodynamic model of membrane humidifiers for pem fuel cell humidification control". *Transaction of the ASME Journal of Dynamic Systems, Measurement and Control,* **127**.

[17] Shimanuki, H., Katagiri, T., Suzuki, M., and Kusano, Y., 2002. "Humidifier for use with a fuel cell". *U.S. Patent number 6471195*.

[18] Choi, K., Park, D., Rho, Y., Kho, Y., and Lee, T., 1998. "A study of the internal humidification of an integrated pemfc stack". *Journal of Power Sources,* **74**.

[19] Mueller, E., and Stefanopoulou, A., 2005. "Analysis, modeling, and validation for the thermal dynamics of a polymer electrolyte membrane fuel cell systems". In Proceedings of the ASME 3rd International Conference on Fuel Cell Science, Engineering and Technology.

[20] Staschewski, D., 1996. "Internal humidifying of pem fuel cells". *International Journal of Hydrogen Energy,* **21**(5).

[21] McKay, D., Stefanopoulou, A., and Cook, J., 2010. "A controllable membrane-type humidifier for fuel cell applications, part 1: operation, modeling and experimental validation". *Journal of Fuel Cell Science and Technology,* **7**(4).

[22] Reid, R., 2002. "Humidification of a pem fuel cell by air-air moisture". *U.S. Patent number 6403249*.

[23] Ramasamy, R., Kumbur, E., Mench, M., Liu, W., Moore, D., and Murthy, M., 2008. "Investigation of macro- and micro-porous layer interaction in polymer electrolyte fuel cells". *International Journal of Hydrogen Energy,* **33**.

[24] Joseph, S., McClure, J., Sebastian, P., Moreira, J., and Valenzuela, E., 2008. "Polyaniline and polypyrrole coatings on aluminum for pem fuel cell bipolar plates". *Journal of Power Sources,* **177**(1).

[25] Hodgson, D., May, B., Adcock, P., and Davies, D., 2001. "New lightweight bipolar plate system for polymer electrolyte membrane fuel cells". *Journal of Power Sources,* **96**(1).

[26] Hsieh, S.-S., Huang, Y.-J., and Her, B.-S., 2009. "Pressure drop on water accumulation distribution for a micro pem fuel cell with different flow field plates". *International Journal of Heat and Mass Transfer,* **52**.

[27] Nguyen, N.-T., and Chan, S., 2006. "Micromachined polymer electrolyte membrane and direct methanol fuel cells - a review". *Journal of Micromechanics and Microengineering,* **16**.

[28] Kumbur, E., Sharp, K., and Mench, M., 2006. "Liquid droplet behaviour and instability in a polymer electrolyte fuel cell flow channel". *Journal of Power Sources,* **161**.

[29] Natarajan, D., and Nguyen, T., 2005. "Curent distribution in pem fuel cells. part 1: Oxygen and fuel flow rate effects". *AIChE Journal,* **51**(9).

[30] O'Hayre, R. P., Cha, S.-W., Colella, W., and Prinz, F. B., 2006. *Fuel Cell Fundamentals*. Wiley, Hoboken, NJ.

[31] Barbir, F., 2005. *PEM Fuel Cells: Theory and Practice*. Elsevier, Burlington, Ma.

[32] Springer, T., Zawodzinski, T., and Gottesfeld, S., 1991. "Polymer electrolyte fuel cell model". *Journal of the Electrochemical Society,* **138**(8).